Measurement of the $\bar{B}_s^0$ Effective Lifetime in the $J/\psi f_0(980)$ Final State

R. Aaij *et al.**
(LHCb Collaboration)

(Received 3 July 2012; published 9 October 2012)

The effective lifetime of the $\bar{B}_s^0$ meson in the decay mode $\bar{B}_s^0 \to J/\psi f_0(980)$ is measured using 1.0 fb^{-1} of data collected in pp collisions at $\sqrt{s} = 7$ TeV with the LHCb detector. The result is $1.700 \pm 0.040 \pm 0.026$ ps, where the first uncertainty is statistical and the second systematic. As the final state is CP-odd, and CP violation in this mode is measured to be small, the lifetime measurement can be translated into a measurement of the decay width of the heavy $\bar{B}_s^0$ mass eigenstate, $\Gamma_H = 0.588 \pm 0.014 \pm 0.009$ ps^{-1}.

DOI: 10.1103/PhysRevLett.109.152002 PACS numbers: 14.40.Nd, 13.25.Hw

The decay $\bar{B}_s^0 \to J/\psi f_0(980)$, $f_0(980) \to \pi^+\pi^-$, discovered by LHCb [1] at close to the predicted rate [2], is important for CP violation [3] and lifetime studies. In this Letter, we make a precise determination of the lifetime. The $J/\psi f_0(980)$ final state is CP-odd, and in the absence of CP violation, can be produced only by the decay of the heavy (H), and not by the light (L), $\bar{B}_s^0$ mass eigenstate [4]. As the measured CP violation in this final state is small [5], a measurement of the effective lifetime, $\tau_{J/\psi f_0}$, can be translated into a measurement of the decay width, Γ_H. This helps to determine the decay width difference, $\Delta\Gamma_s = \Gamma_L - \Gamma_H$, a number of considerable interest for studies of physics beyond the standard model (SM) [6]. Furthermore, this measurement can be used as a constraint in the fit that determines the mixing-induced CP-violating phase in $\bar{B}_s^0$ decays, ϕ_s, using the $J/\psi\phi$ and $J/\psi f_0(980)$ final states, and thus improve the accuracy of the ϕ_s determination [5,7]. In the SM, if subleading penguin contributions are neglected, $\phi_s = -2\arg[\frac{V_{ts}V_{tb}^*}{V_{cs}V_{cb}^*}]$, where the V_{ij} are the Cabibbo-Kobayashi-Maskawa matrix elements, which has a value of $-0.036^{+0.0016}_{-0.0015}$ rad [8]. Note that the LHCb measurement of ϕ_s [5] corresponds to a limit on $\cos\phi_s$ greater than 0.99 at 95% confidence level, consistent with the SM prediction.

The decay time evolution for the sum of B_s^0 and $\bar{B}_s^0$ decays, via the $b \to c\bar{c}s$ tree amplitude, to a CP-odd final state, f_-, is given by [9]

$$\Gamma(B_s^0 \to f_-) + \Gamma(\bar{B}_s^0 \to f_-) = \frac{\mathcal{N}}{2} e^{-\Gamma_s t}\{e^{\Delta\Gamma_s t/2}(1+\cos\phi_s) + e^{-\Delta\Gamma_s t/2}(1-\cos\phi_s)\}, \quad (1)$$

where $\mathcal{N}$ is a time-independent normalization factor and Γ_s is the average decay width. We measure the *effective lifetime* by describing the decay time distribution with a single exponential function

$$\Gamma(B_s^0 \to f_-) + \Gamma(\bar{B}_s^0 \to f_-) = \mathcal{N} e^{-t/\tau_{J/\psi f_0}}. \quad (2)$$

Our procedure involves measuring the lifetime with respect to the well-measured $\bar{B}^0$ lifetime, in the decay mode $\bar{B}^0 \to J/\psi \bar{K}^{*0}$, $\bar{K}^{*0} \to K^-\pi^+$ (the inclusion of charge conjugate modes is implied throughout this Letter). In this ratio, the systematic uncertainties largely cancel.

The data sample consists of 1.0 fb^{-1} of integrated luminosity collected with the LHCb detector [10] in pp collisions at the LHC with 7 TeV center-of-mass energy. The detector is a single-arm forward spectrometer covering the pseudorapidity range $2 < \eta < 5$, designed for the study of particles containing b or c quarks. The detector includes a high-precision tracking system consisting of a silicon-strip vertex detector surrounding the pp interaction region, a large-area silicon-strip detector located upstream of a dipole magnet and three stations of silicon-strip detectors and straw drift-tubes placed downstream. Charged hadrons are identified using two ring-imaging Cherenkov (RICH) detectors. Muons are identified by a muon system composed of alternating layers of iron and multiwire proportional chambers. The trigger consists of a hardware stage, based on information from the calorimeter and muon systems, followed by a software stage that applies a full event reconstruction. The simulated events used in this analysis are generated using PYTHIA 6.4 [11] with a specific LHCb configuration [12], where decays of hadronic particles are described by EVTGEN [13], and the LHCb detector simulation [14] based on GEANT4 [15].

The selection criteria we use for this analysis are the same as those used to measure ϕ_s in $\bar{B}_s^0 \to J/\psi\pi^+\pi^-$ decays [16]. Events are triggered by a $J/\psi \to \mu^+\mu^-$ decay, requiring two identified muons with opposite charge, transverse momentum greater than 500 MeV (we work in units where $c = \hbar = 1$), invariant mass within 120 MeV of the J/ψ mass [17], and form a vertex with a

*Full author list given at the end of the article.

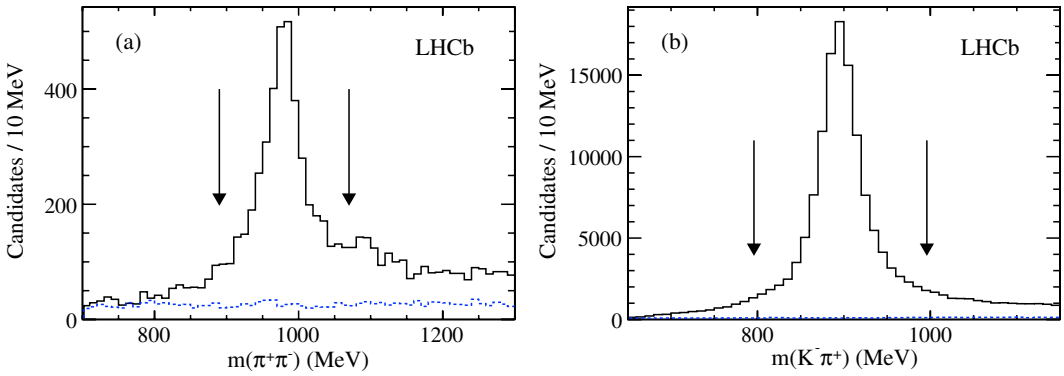

FIG. 1 (color online). Invariant mass distributions of selected (a) $\pi^+\pi^-$ and (b) $K^-\pi^+$ combinations (solid histograms) for events within ± 20 MeV of the respective $\bar{B}_s^0$ and $\bar{B}^0$ mass peaks. Backgrounds (dashed histograms) are determined by fitting the $J/\psi\pi^+\pi^-$ ($J/\psi K^-\pi^+$) mass in bins of $\pi^+\pi^-$ ($K^-\pi^+$) mass. Regions between the arrows are used in the subsequent analysis.

fit χ^2 less than 16. $J/\psi\pi^+\pi^-$ candidates are first selected by pairing an opposite sign pion combination with a J/ψ candidate that has a dimuon invariant mass from -48 MeV to $+43$ MeV from the J/ψ mass [17]. The pions are required to be identified positively in the RICH detector, have a minimum distance of approach with respect to the primary vertex (impact parameter) of greater than 9 standard deviation significance, have a transverse momentum greater than 250 MeV, and fit to a common vertex with the J/ψ with a χ^2 less than 16. Furthermore, the $J/\psi\pi^+\pi^-$ candidate must have a vertex with a fit χ^2 less than 10, flight distance from production to decay vertex greater than 1.5 mm, and the angle between the combined momentum vector of the decay products and the vector formed from the positions of the primary and the $\bar{B}_s^0$ decay vertices (pointing angle) is required to be consistent with zero. Events satisfying this preselection are then further filtered using requirements determined using a boosted decision tree (BDT) [18]. The BDT uses nine variables to differentiate signal from background: the identification quality of each muon, the probability that each pion comes from the primary vertex, the transverse momentum of each pion, the $\bar{B}_s^0$ vertex fit quality, flight distance from production to decay vertex, and pointing angle. It is trained with simulated $\bar{B}_s^0 \to J/\psi f_0(980)$ signal events and two background samples from data, the first with like-sign pions with $J/\psi\pi^\pm\pi^\pm$ mass within ± 50 MeV of the $\bar{B}_s^0$ mass and the second from the $\bar{B}_s^0$ upper mass sideband with $J/\psi\pi^+\pi^-$ mass between 200 and 250 MeV above the $\bar{B}_s^0$ mass.

As the effective $\bar{B}_s^0 \to J/\psi f_0(980)$ lifetime is measured relative to that of the decay $\bar{B}^0 \to J/\psi\bar{K}^{*0}$, we use the same trigger, preselection, and BDT to select $J/\psi K^-\pi^+$ events, except for the hadron identification that is applied independently of the BDT. The selected $\pi^+\pi^-$ and $K^-\pi^+$ invariant mass distributions, for candidates with $J/\psi\pi^+\pi^-$ ($J/\psi K^-\pi^+$) mass within ± 20 MeV of the respective B mass peaks are shown in Fig. 1. The background distributions shown are determined by fitting the $J/\psi\pi^+\pi^-$ ($J/\psi K^-\pi^+$) mass distribution in bins of $\pi^+\pi^-$ ($K^-\pi^+$) mass. Further selections of ± 90 MeV around the $f_0(980)$ mass and ± 100 MeV around the $\bar{K}^{*0}$ mass are applied. The $f_0(980)$ selection results in a $\bar{B}_s^0 \to J/\psi f_0(980)$ sample that is greater than 99.4% CP-odd at 95% confidence level [19].

The analysis exploits the fact that the kinematic properties of the $\bar{B}_s^0 \to J/\psi f_0(980)$ decay are very similar to those of the $\bar{B}^0 \to J/\psi\bar{K}^{*0}$ decay. We can select B mesons in either channel using identical kinematic constraints and hence the decay time acceptance introduced by the trigger, reconstruction, and selection requirements should almost cancel in the ratio of the decay time distributions. Therefore, we can determine the $\bar{B}_s^0 \to J/\psi f_0(980)$ lifetime, $\tau_{J/\psi f_0}$, relative to the $\bar{B}^0 \to J/\psi\bar{K}^{*0}$ lifetime, $\tau_{J/\psi\bar{K}^{*0}}$, from the variation of the ratio of the B meson yields with decay time

$$R(t) = R(0)e^{-t(1/\tau_{J/\psi f_0} - 1/\tau_{J/\psi\bar{K}^{*0}})} = R(0)e^{-t\Delta_{J/\psi f_0}}, \quad (3)$$

where the width difference $\Delta_{J/\psi f_0} = 1/\tau_{J/\psi f_0} - 1/\tau_{J/\psi\bar{K}^{*0}}$.

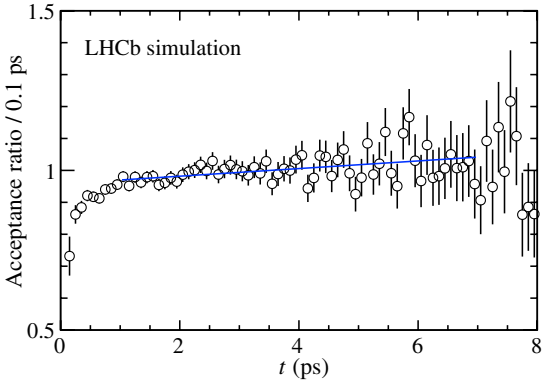

FIG. 2 (color online). Ratio of decay time acceptances between $\bar{B}_s^0 \to J/\psi f_0(980)$ and $\bar{B}^0 \to J/\psi\bar{K}^{*0}$ decays obtained from simulation. The solid (blue) line shows the result of a linear fit.

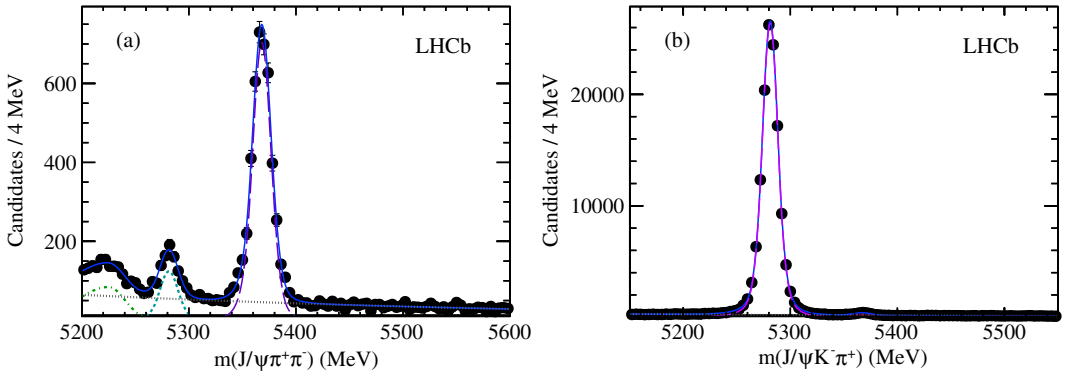

FIG. 3 (color online). Invariant mass distributions of selected (a) $J/\psi\pi^+\pi^-$ and (b) $J/\psi K^-\pi^+$ candidates. The solid (blue) curves show the total fits, the long dashed (purple) curves show the respective $\bar{B}_s^0 \to J/\psi f_0(980)$ and $\bar{B}^0 \to J/\psi \bar{K}^{*0}$ signals, and the dotted (gray) curve shows the combinatorial background. In (a) the short dashed (light blue-green) curve shows the $\bar{B}^0 \to J/\psi\pi^+\pi^-$ background and the dash dotted (green) curve shows the $\bar{B}^0 \to J/\psi K^-\pi^+$ reflection. In (b) the short dashed (red) curve near 5370 MeV shows the $\bar{B}_s^0 \to J/\psi K^-\pi^+$ background.

We test the cancellation of acceptance effects using simulated $\bar{B}_s^0 \to J/\psi f_0(980)$ and $\bar{B}^0 \to J/\psi \bar{K}^{*0}$ events. Both the acceptances themselves and also the ratio exhibit the same behavior. Because of the selection requirements, they are equal to 0 at $t = 0$, after which there is a sharp increase, followed by a slow variation for t greater then 1 ps. Based on this, we only use events with t greater than 1 ps in the analysis. To good approximation, the acceptance ratio is linear between 1 and 7 ps, with a slope of $a = 0.0125 \pm 0.0036$ ps^{-1} (see Fig. 2). We use this slope as a correction to Eq. (3) when fitting the measured decay time ratio

$$R(t) = R_0(1 + at)e^{-t\Delta_{J/\psi f_0}}. \quad (4)$$

Differences between the decay time resolutions of the decay modes could affect the decay time ratio. To measure the decay time resolution, we use prompt events containing a J/ψ meson. Such events are found using a dimuon trigger, plus two opposite-charged tracks with similar selection criteria as for $J/\psi\pi^+\pi^-$ ($J/\psi K^-\pi^+$) events, apart from any decay time biasing requirements such as impact parameters and B flight distance, additionally including that the $J/\psi\pi^+\pi^-$ ($J/\psi K^-\pi^+$) mass be within ± 20 MeV of the $\bar{B}_s^0(\bar{B}^0)$ mass. To describe the decay time distribution of these events, we use a triple Gaussian function with a common mean, and two long-lived components, modeled by exponential functions convolved with the triple Gaussian function. The events are dominated by zero lifetime background with the long-lived components comprising less than 5% of the events. We find the average effective decay time resolution for $\bar{B}_s^0 \to J/\psi f_0(980)$ and $\bar{B}^0 \to J/\psi \bar{K}^{*0}$ decays to be 41.0 ± 0.9 fs and 44.1 ± 0.2 fs respectively, where the uncertainties are statistical only. This difference was found not to bias the decay time ratio using simulated experiments.

In order to determine the $\bar{B}_s^0 \to J/\psi f_0(980)$ lifetime, we determine the yield of B mesons for both decay modes using unbinned maximum likelihood fits to the B mass distributions in 15 bins of decay time of equal width between 1 and 7 ps. We perform a χ^2 fit to the ratio of the yields as a function of decay time and determine the relative lifetime according to Eq. (4). We obtain the signal and peaking background shape parameters by fitting the time-integrated data set. In each decay time bin, we use these shapes and determine the combinatorial background parameters from the upper mass sidebands,

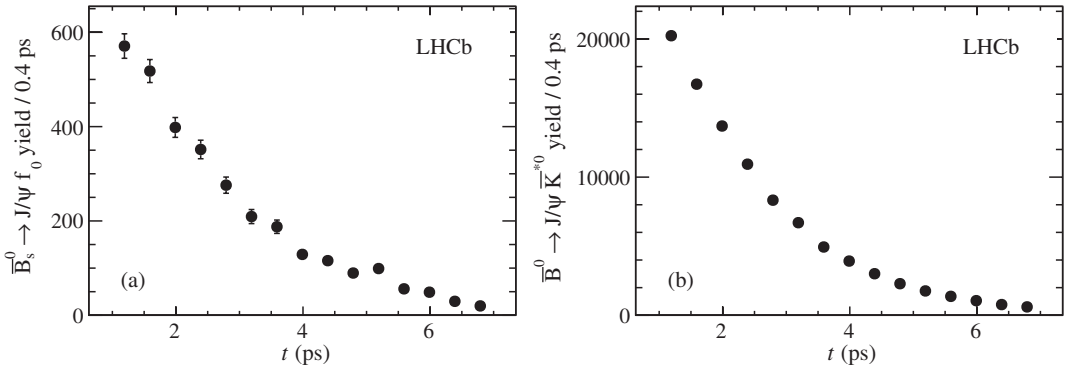

FIG. 4. Decay time distributions for (a) $\bar{B}_s^0 \to J/\psi f_0(980)$ and (b) $\bar{B}^0 \to J/\psi \bar{K}^{*0}$. In (b) the error bars are smaller than the points.

$5450 < m(J/\psi f_0) < 5600\,\text{MeV}$ and $5450 < m(J/\psi \bar{K}^{*0}) < 5550\,\text{MeV}$. With this approach, the combinatorial backgrounds are reevaluated in each bin and we make no assumptions on the shape of the background decay time distributions. This method was tested with high statistics simulated experiments and found to be unbiased.

The time-integrated fits to the $J/\psi f_0(980)$ and the $J/\psi \bar{K}^{*0}$ mass spectra are shown in Fig. 3. The signal distributions are described by the sum of two crystal ball functions [20] with common means and resolutions for the Gaussian core, but different parameters describing the tails

$$f(m;\mu,\sigma,n_{l,r},\alpha_{l,r}) = \begin{cases} \left(\frac{n_l}{|\alpha_l|}\right)^{n_l} \exp\left(\frac{-|\alpha_l|^2}{2}\right)\left(\frac{n_l}{|\alpha_l|} - |\alpha_l| - \frac{|m-\mu|}{\sigma}\right)^{-n_l}, & \text{if } \frac{m-\mu}{\sigma} \le -\alpha_l, \\ \left(\frac{n_r}{|\alpha_r|}\right)^{n_r} \exp\left(\frac{-|\alpha_r|^2}{2}\right)\left(\frac{n_r}{|\alpha_r|} - |\alpha_r| - \frac{|m-\mu|}{\sigma}\right)^{-n_r}, & \text{if } \frac{m-\mu}{\sigma} \ge \alpha_r, \\ \exp\left(\frac{-(m-\mu)^2}{2\sigma^2}\right), & \text{otherwise,} \end{cases} \quad (5)$$

where μ is the mean and σ the width of the core, while $n_{l,r}$ are the exponent of the left and right tails, and $\alpha_{l,r}$ are the left and right transition points between the core and tails. The left-hand tail accounts for final state radiation and interactions with matter, while the right-hand tail describes non-Gaussian detector effects only seen with increased statistics. The combinatorial backgrounds are described by exponential functions. All parameters are determined from data. There are 4040 ± 75 $\bar{B}^0_s \to J/\psi f_0(980)$ and $131\,920 \pm 400$ $\bar{B}^0 \to J/\psi \bar{K}^{*0}$ signal decays. The decay time distributions, determined using fits to the invariant mass distributions in bins of decay time as described above, are shown in Fig. 4. These are made by placing the fitted signal yields at the average $\bar{B}^0 \to J/\psi \bar{K}^{*0}$ decay time within the bin rather than at the center of the decay time bin. This procedure corrects for the exponential decrease of the decay time distributions across the bin. The subsequent decay time ratio distribution is shown in Fig. 5, and the fitted reciprocal lifetime difference is $\Delta_{J/\psi f_0} = -0.070 \pm 0.014\ \text{ps}^{-1}$, where the uncertainty is statistical only. Taking $\tau_{J/\psi \bar{K}^{*0}}$ to be the mean $\bar{B}^0$ lifetime 1.519 ± 0.007 ps [17], we determine $\tau_{J/\psi f_0} = 1.700 \pm 0.040$ ps.

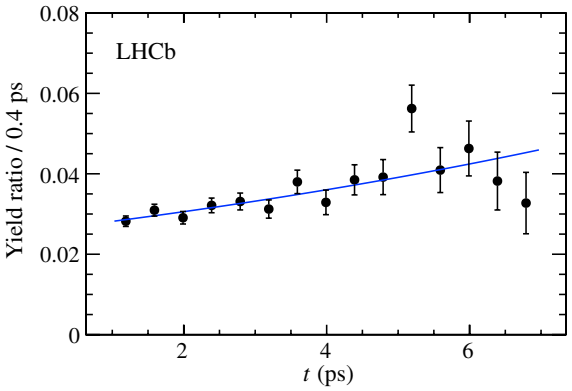

FIG. 5 (color online). Decay time ratio between $\bar{B}^0_s \to J/\psi f_0(980)$ and $\bar{B}^0 \to J/\psi \bar{K}^{*0}$, and the fit for $\Delta_{J/\psi f_0}$.

Sources of systematic uncertainty on the $\bar{B}^0_s \to J/\psi f_0(980)$ lifetime are investigated and listed in Table I. We first investigate our assumptions about the signal and combinatorial background mass shapes. The relative change of the determined $\bar{B}^0_s \to J/\psi f_0(980)$ lifetime between fits with double crystal ball functions and double Gaussian functions for the signal models is 0.001 ps, and between fits with exponential functions and straight lines for the combinatorial background models is 0.010 ps. The different particle identification criteria used to select $\bar{B}^0_s \to J/\psi f_0(980) \to \mu^+\mu^-\pi^+\pi^-$ and $\bar{B}^0 \to J/\psi \bar{K}^{*0} \to \mu^+\mu^- K^-\pi^+$ decays could affect the acceptance cancellation between the modes. In order to investigate this effect, we loosen and tighten the particle identification selection for the kaon, modifying the $\bar{B}^0 \to J/\psi \bar{K}^{*0}$ signal yield by $+2\%$ and -20%, respectively, and repeat the analysis. The larger difference with respect to the default selection, 0.007 ps, is assigned as a systematic uncertainty. We also assign half of the relative change between the fit without the acceptance correction and the default fit, 0.018 ps, as a systematic uncertainty. Potential statistical biases of our method were evaluated with simulated experiments using similar sample sizes to those in data. An average bias of 0.012 ps is seen and included as a systematic uncertainty.

TABLE I. Summary of systematic uncertainties on the $\bar{B}^0_s \to J/\psi f_0(980)$ effective lifetime.

Source	Uncertainty (ps)
Signal mass shape	0.001
Background mass shape	0.010
Kaon identification	0.007
Acceptance	0.018
Statistical bias	0.012
CP-even component	0.001
$\bar{B}^0$ lifetime [17]	0.009
Sum in quadrature	0.026

The observed bias vanishes in simulated experiments with large sample sizes. As a cross-check, the analysis is performed with various decay time bin widths and fit ranges, and consistent results are obtained. The possible CP-even component, limited to be less than 0.6% at 95% confidence level [19], introduces a 0.001 ps systematic uncertainty. Using the Particle Data Group value for the $\bar{B}^0$ lifetime [17] as input requires the propagation of its error as a systematic uncertainty. All the contributions are added in quadrature and yield a total systematic uncertainty on the lifetime of 0.026 ps (1.5%). Thus the effective lifetime of the $J/\psi f_0(980)$ final state in $\bar{B}^0_s$ decays, when describing the decay time distribution as a single exponential, is

$$\tau_{J/\psi f_0} = 1.700 \pm 0.040 \pm 0.026 \text{ ps}. \quad (8)$$

Given that ϕ_s is measured to be small, and the decay is given by a pure $b \to c\bar{c}s$ tree amplitude, we may interpret the inverse of the $\bar{B}^0_s \to J/\psi f_0(980)$ effective lifetime as a measurement of Γ_H with an additional source of systematic uncertainty due to a possible nonzero value of ϕ_s. For $\cos\phi_s = 0.99$, $\Gamma_s = 0.6580$ ps^{-1} and $\Delta\Gamma_s = 0.116$ ps^{-1} [5], $\tau_{J/\psi f_0}$ changes by 0.002 ps. This is added in quadrature to the systematic uncertainties on $\tau_{J/\psi f_0}$ to obtain the final systematic uncertainty on Γ_H.

In summary, the effective lifetime of the $\bar{B}^0_s$ meson in the CP-odd $J/\psi f_0(980)$ final state has been measured with respect to the well-measured $\bar{B}^0$ lifetime in the final state $J/\psi \bar{K}^{*0}$. The analysis exploits the kinematic similarities between the $\bar{B}^0_s \to J/\psi f_0(980)$ and $\bar{B}^0 \to J/\psi \bar{K}^{*0}$ decays to determine an effective lifetime of

$$\tau_{J/\psi f_0} = 1.700 \pm 0.040 \pm 0.026 \text{ ps},$$

corresponding to a width difference of

$$\Delta_{J/\psi f_0} = -0.070 \pm 0.014 \pm 0.001 \text{ ps}^{-1},$$

where the uncertainties are statistical and systematic, respectively. This result is consistent with, and more precise than, the previous measurement of $1.70^{+0.12}_{-0.11} \pm 0.03$ ps from CDF [21]. Interpreting this as the lifetime of the heavy $\bar{B}^0_s$ eigenstate, we obtain

$$\Gamma_H = 0.588 \pm 0.014 \pm 0.009 \text{ ps}^{-1}.$$

This value of Γ_H is consistent with the value 0.600 ± 0.013 ps^{-1}, calculated from the values of Γ_s and $\Delta\Gamma_s$ in Ref. [5].

We express our gratitude to our colleagues in the CERN accelerator departments for the excellent performance of the LHC. We thank the technical and administrative staff at CERN and at the LHCb institutes, and acknowledge support from the national agencies: CAPES, CNPq, FAPERJ, and FINEP (Brazil); CERN; NSFC (China); CNRS/IN2P3 (France); BMBF, DFG, HGF, and MPG (Germany); SFI (Ireland); INFN (Italy); FOM and NWO (The Netherlands); SCSR (Poland); ANCS (Romania); MinES of Russia and Rosatom (Russia); MICINN, XuntaGal, and GENCAT (Spain); SNSF and SER (Switzerland); NAS Ukraine (Ukraine); STFC (United Kingdom); NSF (USA). We also acknowledge the support received from the ERC under FP7 and the Region Auvergne.

[1] R. Aaij *et al.* (LHCb Collaboration), Phys. Lett. B **698**, 115 (2011).
[2] S. Stone and L. Zhang, Phys. Rev. D **79**, 074024 (2009).
[3] R. Aaij *et al.* (LHCb Collaboration), Phys. Lett. B **707**, 497 (2012).
[4] R. Aaij *et al.* (LHCb Collaboration), Phys. Rev. Lett. **108**, 241801 (2012).
[5] LHCb Collaboration, "Tagged Time-Dependent Angular Analysis of $\bar{B}^0_s \to J/\psi\phi$ Decays at LHCb," LHCb-CONF-2012-002, 2012.
[6] M. Freytsis, Z. Ligeti, and S. Turczyk, arXiv:1203.3545; A. Lenz, U. Nierste, J. Charles, S. Descotes-Genon, H. Lacker, S. Monteil, V. Niess, and S. T'Jampens, Phys. Rev. D **86**, 033008 (2012); C. Bobeth and U. Haisch, arXiv:1109.1826.
[7] R. Fleischer and R. Knegjens, Eur. Phys. J. C **71**, 1789 (2011).
[8] J. Charles *et al.*, Phys. Rev. D **84**, 033005 (2011).
[9] U. Nierste, arXiv:0904.1869; I. I. Bigi and A. Sanda, Cambridge Monogr. Part. Phys., Nucl. Phys., Cosmol. **9**, 1 (2000).
[10] A. A. Alves, Jr *et al.* (LHCb Collaboration), JINST **3**, S08005 (2008).
[11] T. Sjöstrand, S. Mrenna, and P. Skands, J. High Energy Phys. 05 (2006) 026.
[12] I. Belyaev *et al.*, *Nuclear Science Symposium Conference Record (NSS/MIC)* (IEEE, New York, 2010), p. 1155
[13] D. J. Lange, Nucl. Instrum. Methods Phys. Res., Sect. A **462**, 152 (2001).
[14] M. Clemencic, G. Corti, S. Easo, C. R. Jones, S. Miglioranzi, M. Pappagallo, and P. Robbe, J. Phys. Conf. Ser. **331**, 032023 (2011).
[15] J. Allison *et al.* (GEANT4 Collaboration), IEEE Trans. Nucl. Sci. **53**, 270 (2006); S. Agostinelli *et al.* (GEANT4 Collaboration), Nucl. Instrum. Methods Phys. Res., Sect. A **506**, 250 (2003).
[16] R. Aaij *et al.* (LHCb Collaboration), Phys. Lett. B **713**, 378 (2012).
[17] J. Beringer *et al.* (Particle Data Group), Phys. Rev. D **86**, 010001 (2012).
[18] B. P. Roe, H.-J. Yang, J. Zhu, Y. Liu, I. Stancu, and G. McGregor, Nucl. Instrum. Methods Phys. Res., Sect. A **543**, 577 (2005).A. Hoecker *et al.*, Proc. Sci., ACAT (**2007**) 040 [arXiv:physics/0703039].
[19] R. Aaij *et al.* (LHCb Collaboration), arXiv:1204.5643 [Phys. Rev. D (to be published)].

[20] T. Skwarnicki, Ph.D. thesis, Institute of Nuclear Physics, Krakow [Institution Report No. DESY-F31-86-02, 1986].

[21] T. Aaltonen *et al.* CDF Collaboration, Phys. Rev. D **84**, 052012 (2011).

R. Aaij,[38] C. Abellan Beteta,[33,a] A. Adametz,[11] B. Adeva,[34] M. Adinolfi,[43] C. Adrover,[6] A. Affolder,[49] Z. Ajaltouni,[5] J. Albrecht,[35] F. Alessio,[35] M. Alexander,[48] S. Ali,[38] G. Alkhazov,[27] P. Alvarez Cartelle,[34] A. A. Alves Jr,[22] S. Amato,[2] Y. Amhis,[36] L. Anderlini,[17] J. Anderson,[37] R. B. Appleby,[51] O. Aquines Gutierrez,[10] F. Archilli,[18,35] A. Artamonov,[32] M. Artuso,[53,35] E. Aslanides,[6] G. Auriemma,[22,b] S. Bachmann,[11] J. J. Back,[45] V. Balagura,[28,35] W. Baldini,[16] R. J. Barlow,[51] C. Barschel,[35] S. Barsuk,[7] W. Barter,[44] A. Bates,[48] C. Bauer,[10] Th. Bauer,[38] A. Bay,[36] J. Beddow,[48] I. Bediaga,[1] S. Belogurov,[28] K. Belous,[32] I. Belyaev,[28] E. Ben-Haim,[8] M. Benayoun,[8] G. Bencivenni,[18] S. Benson,[47] J. Benton,[43] R. Bernet,[37] M.-O. Bettler,[17] M. van Beuzekom,[38] A. Bien,[11] S. Bifani,[12] T. Bird,[51] A. Bizzeti,[17,c] P. M. Bjørnstad,[51] T. Blake,[35] F. Blanc,[36] C. Blanks,[50] J. Blouw,[11] S. Blusk,[53] A. Bobrov,[31] V. Bocci,[22] A. Bondar,[31] N. Bondar,[27] W. Bonivento,[15] S. Borghi,[48,51] A. Borgia,[53] T. J. V. Bowcock,[49] C. Bozzi,[16] T. Brambach,[9] J. van den Brand,[39] J. Bressieux,[36] D. Brett,[51] M. Britsch,[10] T. Britton,[53] N. H. Brook,[43] H. Brown,[49] A. Büchler-Germann,[37] I. Burducea,[26] A. Bursche,[37] J. Buytaert,[35] S. Cadeddu,[15] O. Callot,[7] M. Calvi,[20,d] M. Calvo Gomez,[33,a] A. Camboni,[33] P. Campana,[18,35] A. Carbone,[14] G. Carboni,[21,e] R. Cardinale,[19,35,f] A. Cardini,[15] L. Carson,[50] K. Carvalho Akiba,[2] G. Casse,[49] M. Cattaneo,[35] Ch. Cauet,[9] M. Charles,[52] Ph. Charpentier,[35] P. Chen,[3,36] N. Chiapolini,[37] M. Chrzaszcz,[23] K. Ciba,[35] X. Cid Vidal,[34] G. Ciezarek,[50] P. E. L. Clarke,[47] M. Clemencic,[35] H. V. Cliff,[44] J. Closier,[35] C. Coca,[26] V. Coco,[38] J. Cogan,[6] E. Cogneras,[5] P. Collins,[35] A. Comerma-Montells,[33] A. Contu,[52] A. Cook,[43] M. Coombes,[43] G. Corti,[35] B. Couturier,[35] G. A. Cowan,[36] D. Craik,[45] S. Cunliffe,[50] R. Currie,[47] C. D'Ambrosio,[35] P. David,[8] P. N. Y. David,[38] I. De Bonis,[4] K. De Bruyn,[38] S. De Capua,[21,e] M. De Cian,[37] J. M. De Miranda,[1] L. De Paula,[2] P. De Simone,[18] D. Decamp,[4] M. Deckenhoff,[9] H. Degaudenzi,[36,35] L. Del Buono,[8] C. Deplano,[15] D. Derkach,[14,35] O. Deschamps,[5] F. Dettori,[39] J. Dickens,[44] H. Dijkstra,[35] P. Diniz Batista,[1] F. Domingo Bonal,[33,a] S. Donleavy,[49] F. Dordei,[11] A. Dosil Suárez,[34] D. Dossett,[45] A. Dovbnya,[40] F. Dupertuis,[36] R. Dzhelyadin,[32] A. Dziurda,[23] A. Dzyuba,[27] S. Easo,[46] U. Egede,[50] V. Egorychev,[28] S. Eidelman,[31] D. van Eijk,[38] F. Eisele,[11] S. Eisenhardt,[47] R. Ekelhof,[9] L. Eklund,[48] I. El Rifai,[5] Ch. Elsasser,[37] D. Elsby,[42] D. Esperante Pereira,[34] A. Falabella,[16,14,g] C. Färber,[11] G. Fardell,[47] C. Farinelli,[38] S. Farry,[12] V. Fave,[36] V. Fernandez Albor,[34] F. Ferreira Rodrigues,[1] M. Ferro-Luzzi,[35] S. Filippov,[30] C. Fitzpatrick,[47] M. Fontana,[10] F. Fontanelli,[19,f] R. Forty,[35] O. Francisco,[2] M. Frank,[35] C. Frei,[35] M. Frosini,[17,h] S. Furcas,[20] A. Gallas Torreira,[34] D. Galli,[14,i] M. Gandelman,[2] P. Gandini,[52] Y. Gao,[3] J-C. Garnier,[35] J. Garofoli,[53] J. Garra Tico,[44] L. Garrido,[33] D. Gascon,[33] C. Gaspar,[35] R. Gauld,[52] E. Gersabeck,[11] M. Gersabeck,[35] T. Gershon,[45,35] Ph. Ghez,[4] V. Gibson,[44] V. V. Gligorov,[35] C. Göbel,[54] D. Golubkov,[28] A. Golutvin,[50,28,35] A. Gomes,[2] H. Gordon,[52] M. Grabalosa Gándara,[33] R. Graciani Diaz,[33] L. A. Granado Cardoso,[35] E. Graugés,[33] G. Graziani,[17] A. Grecu,[26] E. Greening,[52] S. Gregson,[44] O. Grünberg,[55] B. Gui,[53] E. Gushchin,[30] Yu. Guz,[32] T. Gys,[35] C. Hadjivasiliou,[53] G. Haefeli,[36] C. Haen,[35] S. C. Haines,[44] S. Hall,[50] T. Hampson,[43] S. Hansmann-Menzemer,[11] N. Harnew,[52] S. T. Harnew,[43] J. Harrison,[51] P. F. Harrison,[45] T. Hartmann,[55] J. He,[7] V. Heijne,[38] K. Hennessy,[49] P. Henrard,[5] J. A. Hernando Morata,[34] E. van Herwijnen,[35] E. Hicks,[49] M. Hoballah,[5] P. Hopchev,[4] W. Hulsbergen,[38] P. Hunt,[52] T. Huse,[49] R. S. Huston,[12] D. Hutchcroft,[49] D. Hynds,[48] V. Iakovenko,[41] P. Ilten,[12] J. Imong,[43] R. Jacobsson,[35] A. Jaeger,[11] M. Jahjah Hussein,[5] E. Jans,[38] F. Jansen,[38] P. Jaton,[36] B. Jean-Marie,[7] F. Jing,[3] M. John,[52] D. Johnson,[52] C. R. Jones,[44] B. Jost,[35] M. Kaballo,[9] S. Kandybei,[40] M. Karacson,[35] T. M. Karbach,[9] J. Keaveney,[12] I. R. Kenyon,[42] U. Kerzel,[35] T. Ketel,[39] A. Keune,[36] B. Khanji,[6] Y. M. Kim,[47] M. Knecht,[36] O. Kochebina,[7] I. Komarov,[29] R. F. Koopman,[39] P. Koppenburg,[38] M. Korolev,[29] A. Kozlinskiy,[38] L. Kravchuk,[30] K. Kreplin,[11] M. Kreps,[45] G. Krocker,[11] P. Krokovny,[31] F. Kruse,[9] M. Kucharczyk,[20,23,35,d] V. Kudryavtsev,[31] T. Kvaratskheliya,[28,35] V. N. La Thi,[36] D. Lacarrere,[35] G. Lafferty,[51] A. Lai,[15] D. Lambert,[47] R. W. Lambert,[39] E. Lanciotti,[35] G. Lanfranchi,[18] C. Langenbruch,[35] T. Latham,[45] C. Lazzeroni,[42] R. Le Gac,[6] J. van Leerdam,[38] J.-P. Lees,[4] R. Lefèvre,[5] A. Leflat,[29,35] J. Lefrançois,[7] O. Leroy,[6] T. Lesiak,[23] L. Li,[3] Y. Li,[3] L. Li Gioi,[5] M. Lieng,[9] M. Liles,[49] R. Lindner,[35] C. Linn,[11] B. Liu,[3] G. Liu,[35] J. von Loeben,[20] J. H. Lopes,[2] E. Lopez Asamar,[33] N. Lopez-March,[36] H. Lu,[3] J. Luisier,[36] A. Mac Raighne,[48] F. Machefert,[7] I. V. Machikhiliyan,[4,28] F. Maciuc,[10] O. Maev,[27,35] J. Magnin,[1] S. Malde,[52] R. M. D. Mamunur,[35] G. Manca,[15,j] G. Mancinelli,[6] N. Mangiafave,[44] U. Marconi,[14] R. Märki,[36] J. Marks,[11] G. Martellotti,[22] A. Martens,[8] L. Martin,[52] A. Martín Sánchez,[7] M. Martinelli,[38] D. Martinez Santos,[35] A. Massafferri,[1] Z. Mathe,[12] C. Matteuzzi,[20] M. Matveev,[27] E. Maurice,[6] A. Mazurov,[16,30,35] J. McCarthy,[42] G. McGregor,[51] R. McNulty,[12] M. Meissner,[11]

M. Merk,[38] J. Merkel,[9] D. A. Milanes,[13] M.-N. Minard,[4] J. Molina Rodriguez,[54] S. Monteil,[5] D. Moran,[12] P. Morawski,[23] R. Mountain,[53] I. Mous,[38] F. Muheim,[47] K. Müller,[37] R. Muresan,[26] B. Muryn,[24] B. Muster,[36] J. Mylroie-Smith,[49] P. Naik,[43] T. Nakada,[36] R. Nandakumar,[46] I. Nasteva,[1] M. Needham,[47] N. Neufeld,[35] A. D. Nguyen,[36] C. Nguyen-Mau,[36,k] M. Nicol,[7] V. Niess,[5] N. Nikitin,[29] T. Nikodem,[11] A. Nomerotski,[52,35] A. Novoselov,[32] A. Oblakowska-Mucha,[24] V. Obraztsov,[32] S. Oggero,[38] S. Ogilvy,[48] O. Okhrimenko,[41] R. Oldeman,[15,35,i] M. Orlandea,[26] J. M. Otalora Goicochea,[2] P. Owen,[50] B. K. Pal,[53] A. Palano,[13,l] M. Palutan,[18] J. Panman,[35] A. Papanestis,[46] M. Pappagallo,[48] C. Parkes,[51] C. J. Parkinson,[50] G. Passaleva,[17] G. D. Patel,[49] M. Patel,[50] G. N. Patrick,[46] C. Patrignani,[19,f] C. Pavel-Nicorescu,[26] A. Pazos Alvarez,[34] A. Pellegrino,[38] G. Penso,[22,m] M. Pepe Altarelli,[35] S. Perazzini,[14,i] D. L. Perego,[20,d] E. Perez Trigo,[34] A. Pérez-Calero Yzquierdo,[33] P. Perret,[5] M. Perrin-Terrin,[6] G. Pessina,[20] A. Petrolini,[19,f] A. Phan,[53] E. Picatoste Olloqui,[33] B. Pie Valls,[33] B. Pietrzyk,[4] T. Pilař,[45] D. Pinci,[22] S. Playfer,[47] M. Plo Casasus,[34] F. Polci,[8] G. Polok,[23] A. Poluektov,[45,31] E. Polycarpo,[2] D. Popov,[10] B. Popovici,[26] C. Potterat,[33] A. Powell,[52] J. Prisciandaro,[36] V. Pugatch,[41] A. Puig Navarro,[33] W. Qian,[53] J. H. Rademacker,[43] B. Rakotomiaramanana,[36] M. S. Rangel,[2] I. Raniuk,[40] N. Rauschmayr,[35] G. Raven,[39] S. Redford,[52] M. M. Reid,[45] A. C. dos Reis,[1] S. Ricciardi,[46] A. Richards,[50] K. Rinnert,[49] D. A. Roa Romero,[5] P. Robbe,[7] E. Rodrigues,[48,51] F. Rodrigues,[2] P. Rodriguez Perez,[34] G. J. Rogers,[44] S. Roiser,[35] V. Romanovsky,[32] A. Romero Vidal,[34] M. Rosello,[33,a] J. Rouvinet,[36] T. Ruf,[35] H. Ruiz,[33] G. Sabatino,[21,e] J. J. Saborido Silva,[34] N. Sagidova,[27] P. Sail,[48] B. Saitta,[15,j] C. Salzmann,[37] B. Sanmartin Sedes,[34] M. Sannino,[19,f] R. Santacesaria,[22] C. Santamarina Rios,[34] R. Santinelli,[35] E. Santovetti,[21,e] M. Sapunov,[6] A. Sarti,[18,d] C. Satriano,[22,b] A. Satta,[21] M. Savrie,[16,g] D. Savrina,[28] P. Schaack,[50] M. Schiller,[39] H. Schindler,[35] S. Schleich,[9] M. Schlupp,[9] M. Schmelling,[10] B. Schmidt,[35] O. Schneider,[36] A. Schopper,[35] M.-H. Schune,[7] R. Schwemmer,[35] B. Sciascia,[18] A. Sciubba,[18,m] M. Seco,[34] A. Semennikov,[28] K. Senderowska,[24] I. Sepp,[50] N. Serra,[37] J. Serrano,[6] P. Seyfert,[11] M. Shapkin,[32] I. Shapoval,[40,35] P. Shatalov,[28] Y. Shcheglov,[27] T. Shears,[49] L. Shekhtman,[31] O. Shevchenko,[40] V. Shevchenko,[28] A. Shires,[50] R. Silva Coutinho,[45] T. Skwarnicki,[53] N. A. Smith,[49] E. Smith,[52,46] M. Smith,[51] K. Sobczak,[5] F. J. P. Soler,[48] A. Solomin,[43] F. Soomro,[18,35] D. Souza,[43] B. Souza De Paula,[2] B. Spaan,[9] A. Sparkes,[47] P. Spradlin,[48] F. Stagni,[35] S. Stahl,[11] O. Steinkamp,[37] S. Stoica,[26] S. Stone,[53,35] B. Storaci,[38] M. Straticiuc,[26] U. Straumann,[37] V. K. Subbiah,[35] S. Swientek,[9] M. Szczekowski,[25] P. Szczypka,[36] T. Szumlak,[24] S. T'Jampens,[4] M. Teklishyn,[7] E. Teodorescu,[26] F. Teubert,[35] C. Thomas,[52] E. Thomas,[35] J. van Tilburg,[11] V. Tisserand,[4] M. Tobin,[37] S. Tolk,[39] S. Topp-Joergensen,[52] N. Torr,[52] E. Tournefier,[4,50] S. Tourneur,[36] M. T. Tran,[36] A. Tsaregorodtsev,[6] N. Tuning,[38] M. Ubeda Garcia,[35] A. Ukleja,[25] U. Uwer,[11] V. Vagnoni,[14] G. Valenti,[14] R. Vazquez Gomez,[33] P. Vazquez Regueiro,[34] S. Vecchi,[16] J. J. Velthuis,[43] M. Veltri,[17,n] G. Veneziano,[36] M. Vesterinen,[35] B. Viaud,[7] I. Videau,[7] D. Vieira,[2] X. Vilasis-Cardona,[33,a] J. Visniakov,[34] A. Vollhardt,[37] D. Volyanskyy,[10] D. Voong,[43] A. Vorobyev,[27] V. Vorobyev,[31] C. Voß,[55] H. Voss,[10] R. Waldi,[55] R. Wallace,[12] S. Wandernoth,[11] J. Wang,[53] D. R. Ward,[44] N. K. Watson,[42] A. D. Webber,[51] D. Websdale,[50] M. Whitehead,[45] J. Wicht,[35] D. Wiedner,[11] L. Wiggers,[38] G. Wilkinson,[52] M. P. Williams,[45,46] M. Williams,[50] F. F. Wilson,[46] J. Wishahi,[9] M. Witek,[23] W. Witzeling,[35] S. A. Wotton,[44] S. Wright,[44] S. Wu,[3] K. Wyllie,[35] Y. Xie,[47] F. Xing,[52] Z. Xing,[53] Z. Yang,[3] R. Young,[47] X. Yuan,[3] O. Yushchenko,[32] M. Zangoli,[14] M. Zavertyaev,[10,o] F. Zhang,[3] L. Zhang,[53] W. C. Zhang,[12] Y. Zhang,[3] A. Zhelezov,[11] L. Zhong,[3] and A. Zvyagin[35]

(LHCb Collaboration)

[1]*Centro Brasileiro de Pesquisas Físicas (CBPF), Rio de Janeiro, Brazil*
[2]*Universidade Federal do Rio de Janeiro (UFRJ), Rio de Janeiro, Brazil*
[3]*Center for High Energy Physics, Tsinghua University, Beijing, China*
[4]*LAPP, Université de Savoie, CNRS/IN2P3, Annecy-Le-Vieux, France*
[5]*Clermont Université, Université Blaise Pascal, CNRS/IN2P3, LPC, Clermont-Ferrand, France*
[6]*CPPM, Aix-Marseille Université, CNRS/IN2P3, Marseille, France*
[7]*LAL, Université Paris-Sud, CNRS/IN2P3, Orsay, France*
[8]*LPNHE, Université Pierre et Marie Curie, Université Paris Diderot, CNRS/IN2P3, Paris, France*
[9]*Fakultät Physik, Technische Universität Dortmund, Dortmund, Germany*
[10]*Max-Planck-Institut für Kernphysik (MPIK), Heidelberg, Germany*
[11]*Physikalisches Institut, Ruprecht-Karls-Universität Heidelberg, Heidelberg, Germany*
[12]*School of Physics, University College Dublin, Dublin, Ireland*
[13]*Sezione INFN di Bari, Bari, Italy*

[14]*Sezione INFN di Bologna, Bologna, Italy*
[15]*Sezione INFN di Cagliari, Cagliari, Italy*
[16]*Sezione INFN di Ferrara, Ferrara, Italy*
[17]*Sezione INFN di Firenze, Firenze, Italy*
[18]*Laboratori Nazionali dell'INFN di Frascati, Frascati, Italy*
[19]*Sezione INFN di Genova, Genova, Italy*
[20]*Sezione INFN di Milano Bicocca, Milano, Italy*
[21]*Sezione INFN di Roma Tor Vergata, Roma, Italy*
[22]*Sezione INFN di Roma La Sapienza, Roma, Italy*
[23]*Henryk Niewodniczanski Institute of Nuclear Physics Polish Academy of Sciences, Kraków, Poland*
[24]*AGH University of Science and Technology, Kraków, Poland*
[25]*Soltan Institute for Nuclear Studies, Warsaw, Poland*
[26]*Horia Hulubei National Institute of Physics and Nuclear Engineering, Bucharest-Magurele, Romania*
[27]*Petersburg Nuclear Physics Institute (PNPI), Gatchina, Russia*
[28]*Institute of Theoretical and Experimental Physics (ITEP), Moscow, Russia*
[29]*Institute of Nuclear Physics, Moscow State University (SINP MSU), Moscow, Russia*
[30]*Institute for Nuclear Research of the Russian Academy of Sciences (INR RAN), Moscow, Russia*
[31]*Budker Institute of Nuclear Physics (SB RAS) and Novosibirsk State University, Novosibirsk, Russia*
[32]*Institute for High Energy Physics (IHEP), Protvino, Russia*
[33]*Universitat de Barcelona, Barcelona, Spain*
[34]*Universidad de Santiago de Compostela, Santiago de Compostela, Spain*
[35]*European Organization for Nuclear Research (CERN), Geneva, Switzerland*
[36]*Ecole Polytechnique Fédérale de Lausanne (EPFL), Lausanne, Switzerland*
[37]*Physik-Institut, Universität Zürich, Zürich, Switzerland*
[38]*Nikhef National Institute for Subatomic Physics, Amsterdam, The Netherlands*
[39]*Nikhef National Institute for Subatomic Physics and VU University Amsterdam, Amsterdam, The Netherlands*
[40]*NSC Kharkiv Institute of Physics and Technology (NSC KIPT), Kharkiv, Ukraine*
[41]*Institute for Nuclear Research of the National Academy of Sciences (KINR), Kyiv, Ukraine*
[42]*University of Birmingham, Birmingham, United Kingdom*
[43]*H.H. Wills Physics Laboratory, University of Bristol, Bristol, United Kingdom*
[44]*Cavendish Laboratory, University of Cambridge, Cambridge, United Kingdom*
[45]*Department of Physics, University of Warwick, Coventry, United Kingdom*
[46]*STFC Rutherford Appleton Laboratory, Didcot, United Kingdom*
[47]*School of Physics and Astronomy, University of Edinburgh, Edinburgh, United Kingdom*
[48]*School of Physics and Astronomy, University of Glasgow, Glasgow, United Kingdom*
[49]*Oliver Lodge Laboratory, University of Liverpool, Liverpool, United Kingdom*
[50]*Imperial College London, London, United Kingdom*
[51]*School of Physics and Astronomy, University of Manchester, Manchester, United Kingdom*
[52]*Department of Physics, University of Oxford, Oxford, United Kingdom*
[53]*Syracuse University, Syracuse, New York, USA*
[54]*Pontifícia Universidade Católica do Rio de Janeiro (PUC-Rio), Rio de Janeiro, Brazil*
[55]*Institut für Physik, Universität Rostock, Rostock, Germany*

[a]LIFAELS, La Salle, Universitat Ramon Llull, Barcelona, Spain.
[b]Università della Basilicata, Potenza, Italy.
[c]Università di Modena e Reggio Emilia, Modena, Italy.
[d]Università di Milano Bicocca, Milano, Italy.
[e]Università di Roma Tor Vergata, Roma, Italy.
[f]Università di Genova, Genova, Italy.
[g]Università di Ferrara, Ferrara, Italy.
[h]Università di Firenze, Firenze, Italy.
[i]Università di Bologna, Bologna, Italy.
[j]Università di Cagliari, Cagliari, Italy.
[k]Hanoi University of Science, Hanoi, Vietnam.
[l]Università di Bari, Bari, Italy.
[m]Università di Roma La Sapienza, Roma, Italy.
[n]Università di Urbino, Urbino, Italy.
[o]P. N. Lebedev Physical Institute, Russian Academy of Science (LPI RAS), Moscow, Russia.